Role of Hydrogen-Spillover in H_2−NO Reaction over Pd-Supported NO_x-Adsorbing Material, MnO_x−CeO_2

Masato Machida,* Daisuke Kurogi, and Tsuyoshi Kijima

Department of Applied Chemistry, Faculty of Engineering, Miyazaki University, 1-1 Gakuenkibanadai Nishi, Miyazaki 889-2192, Japan

Received: June 17, 2002; In Final Form: October 10, 2002

The reactivity of NO_x-adsorbing material, MnO_x−CeO_2, toward H_2 has been studied in the presence of impregnated Pd catalysts by the use of micropulse reactions, in situ DRIFT spectroscopy, and chemisorption experiments. It was found that NO_x adsorbed on Pd/MnO_x−CeO_2 can be largely removed by micropulse H_2 injections at 150 °C, which ensure the conversion of nitrite adsorbates (NO_2^-) into N_2 and thus recover the adsorbability. The results of O_2−H_2 titration evidenced that the role played by Pd is to produce atomic hydrogen, which spills over onto MnO_x−CeO_2 and leads to the reduction of the surface. The amount of spilt-over hydrogen was strongly dependent on temperature and the composition of MnO_x−CeO_2; the equimolar oxide ($0.5MnO_x$−$0.5CeO_2$) exhibited ca. 270-fold larger hydrogen uptake compared to the number of surface Pd atom ($n_H/n_{Pd\,s} = 270$) at 150 °C. The anion vacancies thus formed on MnO_x−CeO_2 could be refilled by oxygen spilt-over from Pd. When H_2 was supplied after saturated by the oxidative NO adsorption at 150 °C, hydrogen spilt-over from Pd caused not only the reduction of nitrite species adsorbed on MnO_x−CeO_2, but also the reaction between the anion vacancy and gaseous NO. Consequently, two types of spillover-assisted mechanisms for NO−H_2 reactions were proposed to explain the reason the reduction of adsorbed nitrite spreads out to the whole surface of MnO_x−CeO_2.

Introduction

Recently, sorptive NO_x removal has been attracting much attention as a novel NO_x-controlling process in an oxidizing atmosphere.[1,2] Several NO_x-adsorbing materials based on alkaline solids, metal oxides, and microporous materials can be applied to remove NO_x from exhaust and store it until the atmosphere turns to reductive, or the temperature ramps. More interesting application of NO_x-adsorbing materials is now directed toward the combination with catalysts. A process alternating NO_x sorption and subsequent catalytic reduction has been developed for automotive emission control system using the so-called "NO_x storage and reduction catalysts".[3,4] In the catalyst system under oxidizing atmosphere, NO is stored into an alkali or alkaline earth component dispersed on the catalyst surface. This is followed by short periods of supplying reducing gas, during which thermal desorption of NO_x and subsequent reduction to N_2 takes place on noble metal catalysts. The NO_x-adsorbing catalysts having integrated structures of adsorption sites and catalytically active sites would be of great interest in numerous applications.[5−8]

In the preceding papers,[9−12] we reported that the binary oxides, MnO_x−CeO_2, with the fluorite-type structure adsorb a large amount of NO to yield nitrite (NO_2^-) and/or nitrate (NO_3^-) on the surface. The oxide is also useful as a support material that allows Pd to catalyze NO−H_2 reactions in the presence of excess O_2.[11] Despite the nonselective character of Pd catalysts toward NO−H_2 reaction, Pd/MnO_x−CeO_2 attained 65% NO-conversion of a stream of 0.08% NO, 2% H_2, and 6% O_2 in He at a low temperature of 150 °C, compared to ca. 30% for Pd/γ-Al_2O_3, the reaction on which was more suppressed by competitive O_2−H_2 reaction. The combination of NO sorbability of MnO_x−CeO_2 and H_2 activation of Pd catalysts was found to give rise to a synergistic effect, thus paving the way to development of NO-adsorbing catalysts for selective deNO_x processes. In the catalyst, NO should be adsorbed oxidatively onto MnO_x−CeO_2,[13] whereas H_2 is activated on the surface of Pd. The selective reduction is therefore dependent on the interaction between hydrogen and NO_x adsorbed on MnO_x−CeO_2.[12]

The focus of the present study is on elucidating the mechanism in the NO−H_2 reactions over Pd catalyst supported on the NO_x-adsorbing material. To obtain information of this type of NO−H_2 interaction, we applied micropulse injection method, in situ DRIFT spectroscopy, and hydrogen chemisorption measurement. It was found that in the presence of impregnated Pd, capable of creating hydrogen-spillover, NO_x adsorbed onto MnO_x−CeO_2 can efficiently be reduced to produce N_2. Conventionally, the synergistic effect on catalytic activity in terms of hydrogen-spillover has been pointed out in catalytic reactions, including hydrogenation and/or dehydrogenation.[14] However, the participation in catalytic NO−H_2 reactions is first found in the present study.

Experimental Section

Preparation and Characterization. Precursors of $n$$MnO_x$−$(1 - n)CeO_2$ (n = 0, 0.25, 0.5, and 1.0) were prepared by precipitation from aqueous solutions of nitrates.[10] Calculated amounts of $Mn(NO_3)_2{\cdot}6H_2O$ and/or $Ce(NO_3)_3{\cdot}6H_2O$ (Wako Chemicals, Guaranteed reagent grade) were dissolved in distilled water. Addition of aqueous ammonia solution dropwise to the solution produced a precipitate, which was evaporated to dryness and subsequently calcined at 450 °C for 5 h in air. The supported

* Corresponding author. Tel: +81-985-58-7323. Fax: +81-985-58-7312. E-mail: machida@material.chem.miyazaki-u.ac.jp.

10.1021/jp026321+ CCC: $25.00
Published on Web 12/07/2002

Pd catalysts were prepared by incipient wetness impregnation using an aqueous solution of $Pd(NO_3)_2$ and subsequent calcination at 450 °C for 5 h (0.1, 0.5, and 1.0 wt % loading as Pd). As prepared powder catalysts were pressed and crushed into 20 mesh granules and heated at 400 °C in flowing 20% O_2/He or 5% H_2/He for 1 h before use. These catalysts were denoted as the oxidized catalyst and the reduced catalyst. Pd3d XPS measurement (Shimadzu-Kratos AXIS−HS, Mg Kα, 15kV) demonstrated that the surface Pd species in the oxidized and reduced catalysts were in the form of oxide (PdO) and metal (Pd), respectively. Crystal structure of calcined samples was determined by powder X-ray diffraction (XRD, Shimadzu XD-D1) using monochromated Cu Kα radiation (30 kV, 30 mA). The BET surface area was obtained by measuring N_2 adsorption isotherms at −196 °C.

H_2 Pulse Injection during NO Sorption. The reactivity of adsorbed NO_x to H_2 was evaluated in pulse mode reactions. After the reduction or oxidation treatment, the granular sample (0.2 g) was placed in a stream of NO_x (0.08% NO, 0−10% O_2 balanced with He, $W/F = 0.24$ s g/cm^3) at 150 °C. After the effluent NO_x increased toward the saturation of sorption, 1 cm^3 of H_2 was injected into the stream just before the catalyst bed every 10−20 min. NO_x (NO/NO_2) and other gas species in the effluent were monitored by using a chemiluminescence NO_x analyzer (Shimadzu NOA-305) and a mass spectrometer (LEDA-MASS).

In situ FT-IR. FT-IR spectra of NO_x species adsorbed on Pd/MnO_x-CeO_2 were recorded on a Jasco FT-IR610 spectrometer. A temperature-controllable diffuse reflectance reaction cell (Jasco DR600A) was connected to a gas flow system and a vacuum line. The powder sample (reduced catalyst) was exposed to the reaction gas containing 0.08% NO, 2% O_2, and He balance at 150 °C for 30 min. This was followed by treatment at 150 °C for 10 min in a flowing 1% H_2/He balance and, subsequently, second NO sorption at 150 °C. After each treatment, spectra were recorded in a flowing He at ambient temperature.

Adsorption Measurement. The Pd dispersion of reduced catalysts was determined by a pulsed-flow CO chemisorption method.[15,16] After the reduction treatment and subsequent evacuation, Pd-loaded sample was placed in flowing He to conduct CO injections into the stream just before the catalyst bed. The effluent CO was quantified by using a TCD cell to determine the number of CO molecules chemisorbed onto Pd (n_{CO}). The number of Pd atoms exposed on the surface ($n_{Pd\,s}$) was calculated on assuming the ratio, $n_{CO}/n_{Pd\,s}$, to be unity.[16] The adsorption of H_2 was determined by O_2-H_2 titration, using the pulsed flow technique.[17,18] The reduced catalyst was placed in flowing He at 30 °C, where titration was carried out first with O_2, then with H_2, and finally with O_2 again. For Pd supported on Mn-containing samples, the uptake of O_2 during the first titration was greater than the uptake during the second titration, suggesting that the O_2 uptake during the first titration is mainly used to refill anion vacancies formed in the bulk oxide after reduction at 400 °C. By contrast, a small amount of the anion vacancies near the oxide surface would only be reformed by H_2 titration at 30 or 150 °C. In this case, therefore, the uptake of O_2 was determined from the second titer. The O_2-H_2 titration was also carried out at 150 °C for the comparison with the results of $NO-H_2$ pulse reactions.

Results and Discussion

Structure and NO Uptake of MnO_x-CeO_2. The equimolar binary oxide, $0.5MnO_x-0.5CeO_2$, with the fluorite-type structure exhibits a large NO uptake at low temperatures (<200 °C).[9−11] In this section, the relationship between structure and NO adsorption property of the MnO_x-CeO_2 system is briefly summarized for the latter discussion. Table 1 shows several characteristic parameters concerning NO adsorption onto $0.5MnO_x-0.5CeO_2$. The NO uptake per unit surface is estimated to be 0.95 molecule nm^{-2} from BET surface area and adsorptive NO uptake at 150 °C. Considering the Mn/Ce ratio on the surface, ($n_{Mn\,s}/n_{Ce\,s}$), to be unity as was revealed by XPS,[9] it is suggested that ca. 30% of Ce sites exposed on the surface are occupied by NO_x. The coverage increases at decreasing temperatures to exceed 50% at 30 °C. Such a large coverage is due to not only the basicity of Ce, but also the high catalytic ability of MnO_x also plays a key role in the oxidation of NO to NO_2^-/NO_3^-. Impregnating Pd catalysts increased the NO uptake in the presence of 2% O_2 (Pd-loaded: 0.14 mmol g^{-1}, unloaded: 0.10 mmol g^{-1}), since the oxidative adsorption of NO is further accelerated. Nevertheless, the effect does not mean the significant adsorption of NO_x onto Pd particles. As described later, the dispersion of Pd (1 wt %) impregnated onto $0.5MnO_x-0.5CeO_2$ was only 0.05. Assuming the stoichiometric adsorption, $n_{NO}/n_{Pd\,s} = 1$, the monolayer chemisorption can be estimated to be 4.65 μmol (g-cat)$^{-1}$, which is less than 5% of the amount of adsorption onto $0.5MnO_x-0.5CeO_2$. The large fraction of NO uptake for the Pd-loaded catalyst is therefore ascribable to the oxidative adsorption onto MnO_x-CeO_2.

TABLE 1: Adsorption Properties of $0.5MnO_x-0.5CeO_2$

BET surface area	64 m^2 g^{-1}
NO uptake[a]	0.10 mmol g^{-1}
n_{NO}[b]	0.95 molecule nm^{-2}
$n_{Ce\,s}$[c]	3.25 nm^{-2}
$n_{Mn\,s}/n_{Ce\,s}$[d]	1.0
$n_{NO\,s}/n_{Ce\,s}$	0.3
NO species	NO_2^-/NO_3^-

[a] Determined by measuring a breakthrough curve at 150 °C. 0.08%NO, 10%O_2, He balance. [b] (NO uptake)/surface area. [c] The number of surface Ce averaged on (100), (110), and (111) planes. [d] Ratio on the surface determined by XPS analysis.

Reactivity of Adsorbed NO_x to H_2. The reactivity of adsorbed NO_x toward H_2 was evaluated by the method of micropulse injection of H_2. In this measurement, 1 wt % $Pd/0.5MnO_x-0.5CeO_2$ (reduced catalyst) was placed in a flowing gas mixture (0.08% NO, 0−10% O_2, and He balance) at 150 °C with monitoring NO_x concentration in the reactor effluent as shown in Figure 1. In the presence of O_2 (2% and 10% in the gas feed), the incremental concentration from the beginning of the reaction corresponds to a breakthrough curve of NO adsorption, because no nitrogen compounds except NO/NO_2 were detected in the effluent. In the absence of O_2, on the other hand, a substantial amount of N_2 was evolved at the beginning, suggesting that the reoxidation of $0.5MnO_x-0.5CeO_2$ by NO took place. This is the reason the first breakthrough was prolonged as depicted in the bottom of Figure 1. It should be noted that the same amount of N_2 evolution was also yielded over Pd-unloaded MnO_x-CeO_2 after the reduction treatment. This means that Pd catalyst is not necessary for the reoxidation of MnO_x-CeO_2 by NO at 150 °C.

After the saturation of NO adsorption, the injection of 1 cm^3 of H_2 into the gas feed was repeated (indicated as arrows in the Figure 1). The injection of H_2 immediately gave a sharp but small NO_x desorption followed by a steep drop of the NO_x concentration. The NO_x concentration was then increased slowly again as was observed before the first H_2 pulse. The injections of H_2 after second pulsing also yielded a similar response.

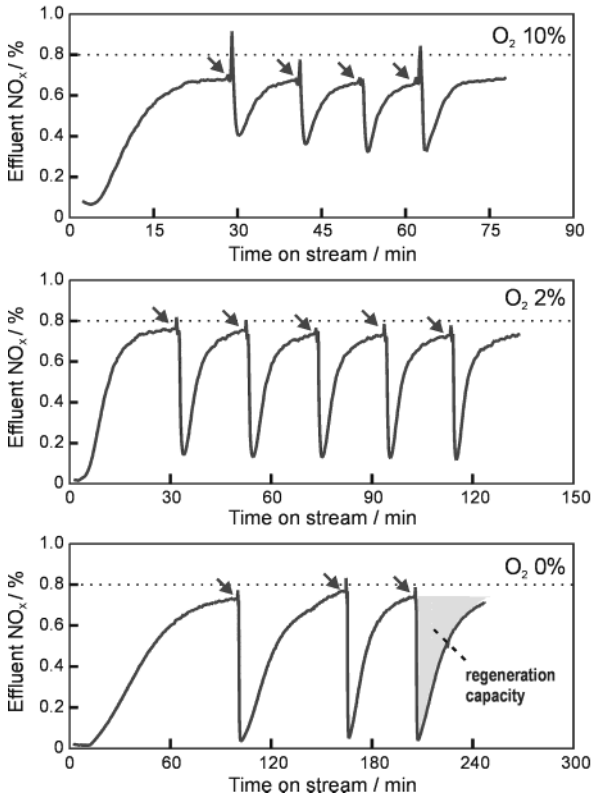

Figure 1. Effect of H_2 pulses on effluent NO from 1 wt % Pd/MnO_x-CeO_2 at 150 °C. Each H_2 pulse was 1.0 cm^3. Gas feed: 0.08% NO, 0, 2, or 10% O_2, He balance, catalyst 0.2 g, $W/F = 0.24$ g s cm^{-3}.

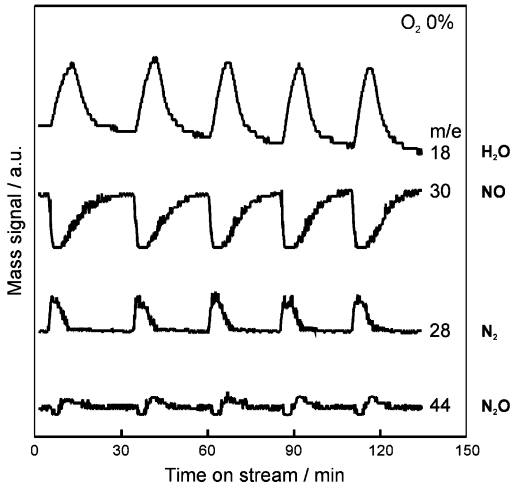

Figure 2. A typical mass signal profile of H_2 pulse reaction at 150 °C. Each H_2 pulse was 1.0 cm^3. Gas feed: 0.08% NO, He balance, catalyst 0.2 g, $W/F = 0.24$ g s cm^{-3}.

During the pulse reactions, the most significant mass fragments were simultaneously monitored to detect the species outcoming from the reactor. The *m*/*e* values, characteristic of the various species, were chosen as 18(H_2O), 30(NO), 28(N_2), and 44(N_2O). The signal of 46(NO_2) was negligibly small and no NH_3 was formed in this $NO-H_2$ reaction.[11] Figure 2 exhibits a typical profile of mass spectral analyses of the effluent gas. Clearly, the injection of H_2 yielded a sharp decrease of signal $m/e = 30$, corresponding to NO, which was synchronized with increases of H_2O, N_2, and N_2O. The mass balance for nitrogen was estimated to be ca. 90%. This apparently suggests the occurrence of the reaction between NO_x adsorbed onto MnO_x-CeO_2 and hydrogen activated on Pd to produce mainly N_2.

Here, we define the adsorptive NO uptake after each H_2 pulse as "regeneration capacity" as shown in Figure 1. Figure 3 compares the regeneration capacity between reduced and oxidized catalysts at different O_2 concentrations in the gas feed. Note that the regeneration capacity for the oxidized catalyst increased with the number of pulsing. This means that part of H_2 injected was consumed to reduce PdO as well as $0.5MnO_x-0.5CeO_2$. On approaching a steady oxidation state after the third pulsing, the regeneration capacity in both cases became almost the same. Regardless of the catalyst pretreatment, the largest regeneration capacity (ca. 0.1 mmol g^{-1}) was obtained for the pulse reaction in the absence of O_2. This is about 20-fold for the amount of monolayer chemisorption of NO onto Pd (a dotted line in Figure 3) and is comparable to the maximum NO uptake of $0.5MnO_x-0.5CeO_2$ at 150 °C (Table 1). Assuming the stoichiometric reaction, $2NO_2 + 4H_2 \rightarrow N_2 + 4H_2O$, the regeneration capacity corresponds to ca. 90% selectivity of H_2 in every injection to the reduction of NO_x stored. A large part of H_2 injected was consumed to reduce NO_x species adsorbed on $0.5MnO_x-0.5CeO_2$.

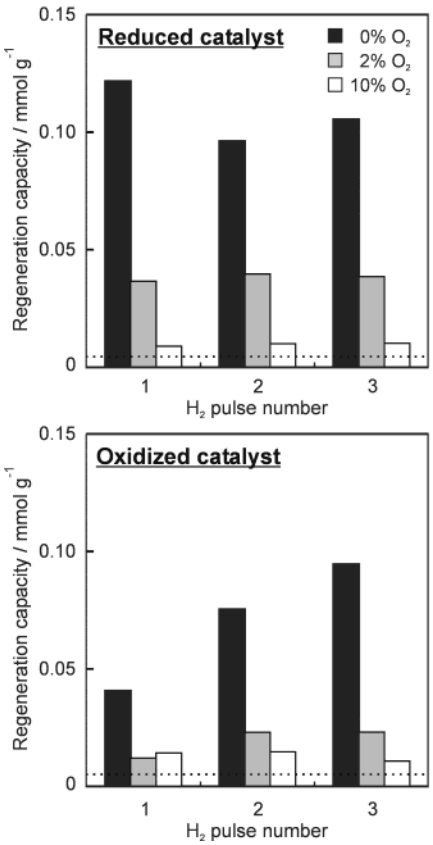

Figure 3. Regeneration capacity of NO adsorption for reduced and oxidized 1 wt % Pd/MnO_x-CeO_2 at 150 °C. The dotted lines correspond to $n_{NO}/n_{Pd\,s} = 1$.

The regeneration capacity decreased with increasing O_2 concentration in the gas feed, suggesting that an incremental part of H_2 injected was reacted with O_2 to produce H_2O. However, it was still larger than the maximum NO uptake onto Pd. Thus, the hydrogen activated on the Pd catalyst could be utilized to reduce NO_x adsorbed on $0.5MnO_x-0.5CeO_2$ even in the presence of excess O_2. The H_2 pulse injection during NO adsorption was also applied to the unloaded $0.5MnO_x-0.5CeO_2$. However, the NO_x breakthrough curve in this case was not influenced by the repeated injection of H_2 pulses. The result is consistent with the view that Pd catalyst to activate H_2 is indispensable for the reduction of NO_x adsorbed on $0.5MnO_x-0.5CeO_2$.

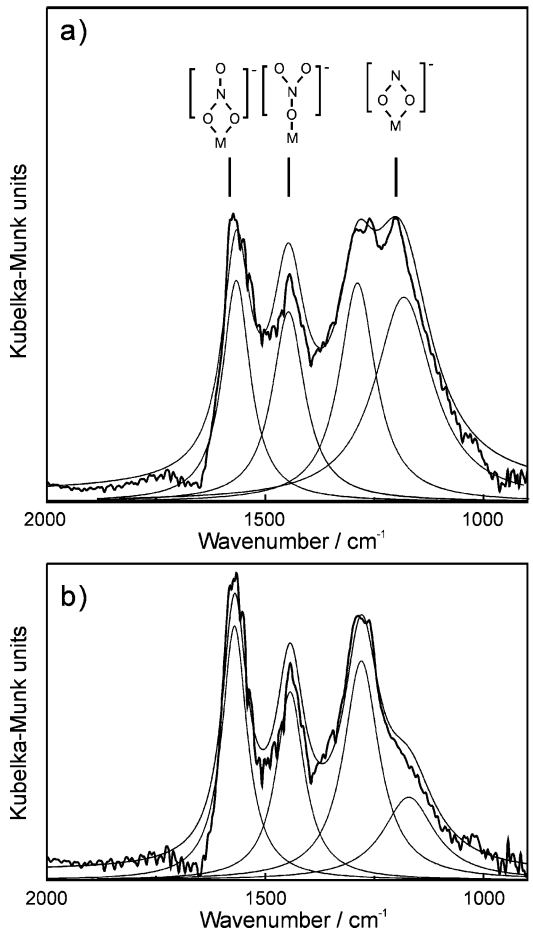

Figure 4. In situ DRIFT spectra of 1 wt % Pd/MnO_x-CeO_2 after (a) exposing to 0.08% NO, 2% O_2/He at 150 °C, and subsequent exposure to (b) 1% H_2/He at 150 °C.

In situ DRIFTS Study. In situ DRIFTS measurement was applied to clarify the structure of NO_x adsorbates on the surface of MnO_x-CeO_2. Figure 4a shows one typical spectrum of 1 wt % $Pd/0.5MnO_x-0.5CeO_2$ taken after NO uptake at 150 °C. The spectrum was characterized by strong bands at 1560, 1440, and 1280 cm^{-1} due to bidentate and unidentate nitrates. It also includes a band of chelating nitrite at 1180 cm^{-1}. These assignments are in accord with those reported previously.[19−23] These bands are much stronger compared with usual Pd-loaded catalysts such as Pd/γ-Al_2O_3, and are very similar to those for NO_2^-/NO_3^- species bound to the surface of MnO_x-CeO_2. The intensity of the bands changed depending upon the oxide composition, reaction temperature, and O_2 concentration in the gas feed.[13] The nitrite species were mainly produced at low O_2 concentration or at ambient temperature, whereas nitrate species became dominant with an increase of O_2 as well as temperature.

Figure 4b exhibits the spectral change after subsequent exposure to a flowing mixture of 1% H_2/He at 150 °C. Clearly, the nitrite band at 1210 cm^{-1} became much less intense after 5 min leaving strong bands of unidentate and bidentate nitrates. The band of nitrite was reversibly restored after subsequent exposure to a stream of NO_x mixture (0.04% NO and 2% O_2/He) at 150 °C. These results suggest that the nitrite species on MnO_x-CeO_2 can be reduced preferentially by H_2 in the presence of Pd catalysts. Similar change of nitrite band was observed in a mixture of 0.25% H_2, 2% O_2, and He balance. During these reactions, the nitrate bands were negligibly affected by H_2, supporting the lower reactivity toward H_2. Indeed, more H_2 (ca. 10% in He) was required to weaken the nitrate bands even in the absence of O_2.

Adsorption Measurement. Table 2 shows O_2/H_2 uptakes measured by O_2-H_2 titration at 30 and 150 °C and resultant adsorption stoichiometries ($n_O/n_{Pd\,s}$, $n_H/n_{Pd\,s}$, and n_H/n_{Pd}). Generally, the O_2-H_2 titration for supported Pd catalysts assumes the following two surface reactions:[17,18]

$$Pd-H + {}^3/_4O_2 \rightarrow Pd-O + {}^1/_2H_2O$$

$$Pd-O + {}^3/_2H_2 \rightarrow Pd-H + H_2O$$

On the basis of the reactions, the surface stoichiometries, $n_O/n_{Pd\,s}$ and $n_H/n_{Pd\,s}$ can be estimated from hydrogen and oxygen titers. When 1 wt % Pd/γ-Al_2O_3 was used as a control catalyst, the H_2 uptake at 30 °C (15.5 μmol (g-cat)$^{-1}$) was close to twice the O_2 uptake (7.8 μmol (g-cat)$^{-1}$) in agreement with the stoichiometry of the above reactions. The resultant $n_H/n_{Pd\,s}$ and $n_O/n_{Pd\,s}$ values were nearly equal to unity as expected.

For unloaded $0.5MnO_x-0.5CeO_2$, the uptake of O_2/H_2 was confirmed to be negligible at 30 and 150 °C. Significant uptakes occurred over 1 wt % $Pd/0.5MnO_x-0.5CeO_2$; $n_H/n_{Pd\,s}$ and $n_O/n_{Pd\,s}$ at 30 °C exceeded 100 (Table 2). The number of hydrogen atoms was still ca. 6-times larger than total number of Pd loaded ($n_H/n_{Pd} = 5.7$). Furthermore, these values were approximately doubled at 150 °C. These results cannot be explained entirely in terms of bulk-type reactions between Pd and O_2/H_2 and

TABLE 2: Adsorption Stoichiometry of Hydrogen and Oxygen

	S_{BET}[a] $m^2 \cdot g^{-1}$	D_{Pd}[b]	temp. °C	uptake μmol g^{-1} [c] O_2	uptake μmol g^{-1} [c] H_2	n_O/n_{Pds}	n_H/n_{Pds}	n_H/n_{Pd}
1 wt %Pd/CeO_2	64	0.27	30	295	120	6.3	7.9	2.1
			150	290	120	6.3	7.7	2.1
1 wt %$Pd/0.25MnO_x-0.75CeO_2$	80	0.05	30	525	225	64	76	3.8
			150	1165	435	124	168	8.4
1 wt %$Pd/0.5MnO_x-0.5CeO_2$	64	0.05	30	795	420	120	114	5.7
			150	1885	835	240	270	13.5
1 wt %Pd/MnO_x	15	0.02	30	220	70	50	79	1.6
			150	810	255	185	290	58
$0.5MnO_x-0.5CeO_2$	64	−	30	0	0	−	−	−
			150	0	0	−	−	−
0.1 wt %$Pd/0.5MnO_x-0.5CeO_2$	64	0.12	150	755	384	460	446	53.5
0.5 wt %$Pd/0.5MnO_x-0.5CeO_2$	64	0.10	150	770	370	106	110	11.0
1 wt %Pd/γ-Al_2O_3	186	0.11	30	7.8	15.5	1.0	1.0	0.1

[a] BET surface area of support oxides. [b] Pd dispersion determined by CO uptake at room temperature. [c] Determined by O_2-H_2 titration.

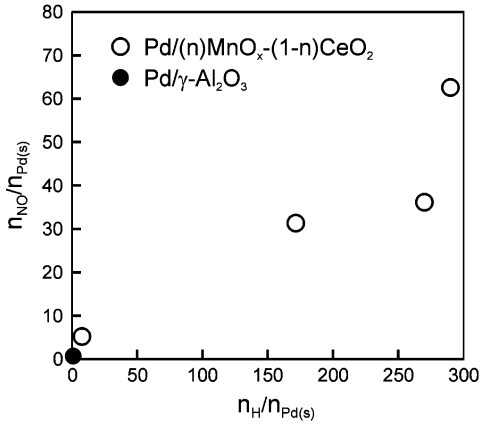

Figure 5. The relationship between $n_{NO}/n_{Pd\,s}$ and $n_H/n_{Pd\,s}$ at 150 °C.

represents the evidence of spillover of hydrogen as well as oxygen onto the support oxides, $0.5MnO_x-0.5CeO_2$. The spillover was also confirmed by measuring the effect of Pd loading on the O_2-H_2 titration at 150 °C, as is also shown in Table 2. Obviously, $n_O/n_{Pd\,s}$ and $n_H/n_{Pd\,s}$ values exceeding 100 even at lower loading amounts (0.1 and 0.5 wt %) are consistent with the spillover of oxygen/hydrogen onto the surface of $0.5MnO_x-0.5CeO_2$. The largest $n_O/n_{Pd\,s}$ and $n_H/n_{Pd\,s}$ values for 0.1 wt % Pd loading may suggest that the spillover is more promoted with a decrease of Pd particle size.

Judging from the elimination of a considerable amount of water after the injection of H_2, the spilt-over hydrogen should remove surface oxygen from $0.5MnO_x-0.5CeO_2$. The surface anion vacancy thus formed was next refilled by spilt-over oxygen. It should be noted that such redox reactions could not take place in the absence of impregnated Pd catalyst at $\leq$150 °C. This means that Pd is capable of accelerating the redox cycles of the MnO_x-CeO_2 binary oxide. It has been suggested that reduction of several metal oxides would be promoted by the occurrence of hydrogen-spillover,[14] because of the higher reactivity of atomic hydrogen compared to molecular hydrogen. For 1 wt % $Pd/0.5MnO_x-0.5CeO_2$ in the present study, the O_2/H_2 uptake at 30°C amounted to 420/795 μmol g^{-1}, which corresponds to 60% surface monolayer of oxygen in the fluorite-type structure. At 150 °C, the uptake implied the lattice oxygen more than surface monolayer takes part in this spillover-assisted redox cycle.

Table 2 suggests that the extent of spillover was dependent on the composition of support oxides. The n_H/n_{Pd} value for Pd/CeO_2 (2.1) was less than that for $Pd/0.5MnO_x-0.5CeO_2$ (5.7). The difference appears to be associated with the redox property of the support oxide. The O_2-TPD measurement in our previous study[9] evidenced increased redox ability caused by Mn-substitution in the present study; O_2 evolution was observed at >300°C for $0.5MnO_x-0.5CeO_2$, compared to >900°C required to unsubstituted CeO_2. The ease of redox would provide a number of surface oxygen sites on the oxide support, which are reactive toward spillover species. On CeO_2, however, such active sites must be much less abundant owing to the lack of redox ability. In this regard, manganese oxide, MnO_x, would be more effective in the induction of spillover. Actually, however, n_H/n_{Pd} obtained for Pd/MnO_x at 30 °C was less than 2, probably because of the lowest surface area of MnO_x (15 m^2 g^{-1}).

Alternative NO/H_2 Pulse Reactions. Figure 5 exhibits the relationship between $n_{NO}/n_{Pd\,s}$ and $n_H/n_{Pd\,s}$ for 1 wt % Pd/MnO_x-CeO_2 and 1 wt % Pd/γ-Al_2O_3 at 150 °C. Here, $n_{NO}/n_{Pd\,s}$ was estimated from the regeneration capacity of NO uptake, which was determined by injecting micropulse H_2 into a flow of 0.08% NO/He as defined in Figure 1. For the Pd/γ-Al_2O_3 catalyst, which showed no evidence for spillover (Table 2), the $n_{NO}/n_{Pd\,s}$ was 0.1, suggesting that the NO adsorption was limited onto the surface of Pd. By contrast, $n_{NO}/n_{Pd\,s}$ much larger than unity was increased with an increase of $n_H/n_{Pd\,s}$ for the Pd/MnO_x-CeO_2 catalysts. This is indicative of the occurrence of the interaction between NO_x adsorbates on MnO_x-CeO_2 and hydrogen spilt-over from Pd.

These results support the hypothesis that hydrogen-spillover plays a key role in attaining the large regeneration capacity ($n_{NO}/n_{Pd\,s}$). However, as yet it is uncertain how NO_x adsorbed on MnO_x-CeO_2 is interacted with spilt-over hydrogen. One possible mechanism is due to the direct reaction between adsorbed NO_x and spilt-over hydrogen, but another mechanism based on the reduction of MnO_x-CeO_2 surface by spilt-over hydrogen followed by the reaction between NO and anion vacancy thus formed is also possible. To determine which mechanism contributes to the large regeneration capacity, alternative NO/H_2 pulse reaction was next applied to the $Pd/0.5MnO_x-0.5CeO_2$ catalyst.

After reduction treatment in 5% H_2/He at 400 °C, 1 wt %$Pd/0.5MnO_x-0.5CeO_2$ was placed in a flow of 1% NO/He at 150 °C for 50 min. Figure 6a exhibits a concentration profile of the effluent measured by a mass spectrometer. The reaction initially produced a large emission of N_2, which was followed by gradual increase of NO reaching toward saturation of NO adsorption onto MnO_x-CeO_2. After changing the gas feed to He, the sample was subjected to pulse reactions. A constant amount (0.68 cm^3) of H_2 and NO were alternatively repeated as shown in Figure 6b. The first H_2 pulse yielded only a very weak N_2 peak ($m/e = 28$), whereas the subsequent NO pulse yielded a N_2 peak with higher intensity. The NO pulse on and after the second injection yielded not only an N_2 but also an N_2O peak ($m/e = 44$). This result is compatible with the reaction between NO and the anion vacancy on the surface of MnO_x-CeO_2. At the end of fourth alternative pulse reactions, the He carrier gas was switched to 1% H_2/He (Figure 6c). Soon after this, a very large N_2 peak appeared, suggesting that the efficient reduction of NO_x adsorbed on MnO_x-CeO_2 could be attained in a flowing H_2/He.

Models for NO$-H_2$ Reaction over Pd/MnO_x-CeO_2. We have to consider the significant reactions between spilt-over hydrogen and NO_x adsorbates stored on the surface of MnO_x-CeO_2, which take place with the assistance of a Pd catalyst. The two possible models for the NO$-H_2$ reaction over Pd/MnO_x-CeO_2 can be proposed as illustrated schematically in Figure 7. The first model is the reaction between gaseous NO and the anion vacancy created by spilt-over hydrogen. The reaction would take place in the vicinity of the boundary with Pd, where anion vacancy must be most abundant. However, it should have no effect on the NO_x adsorbates at a distance from Pd particles. This idea supports data on the alternative pulse reactions (Figure 6b), which indicate that N_2 is yielded when NO was pulsed after the H_2 injection. On the other hand, the second model is based on the direct reduction of NO_x adsorbates by spilt-over hydrogen. This process requires continuous H_2 supply to NO_x-saturated MnO_x-CeO_2, which would expand the reduced area on the surface of MnO_x-CeO_2 and consequently convert a large number of NO_x adsorbates into N_2. Unlike the first case, this reaction is characterized by a very large amount of N_2 formation (Figure 6c). These two reaction paths seem to be responsible for the NO reduction depending on the amount of supplied H_2. When the amount of H_2 is small, the first path

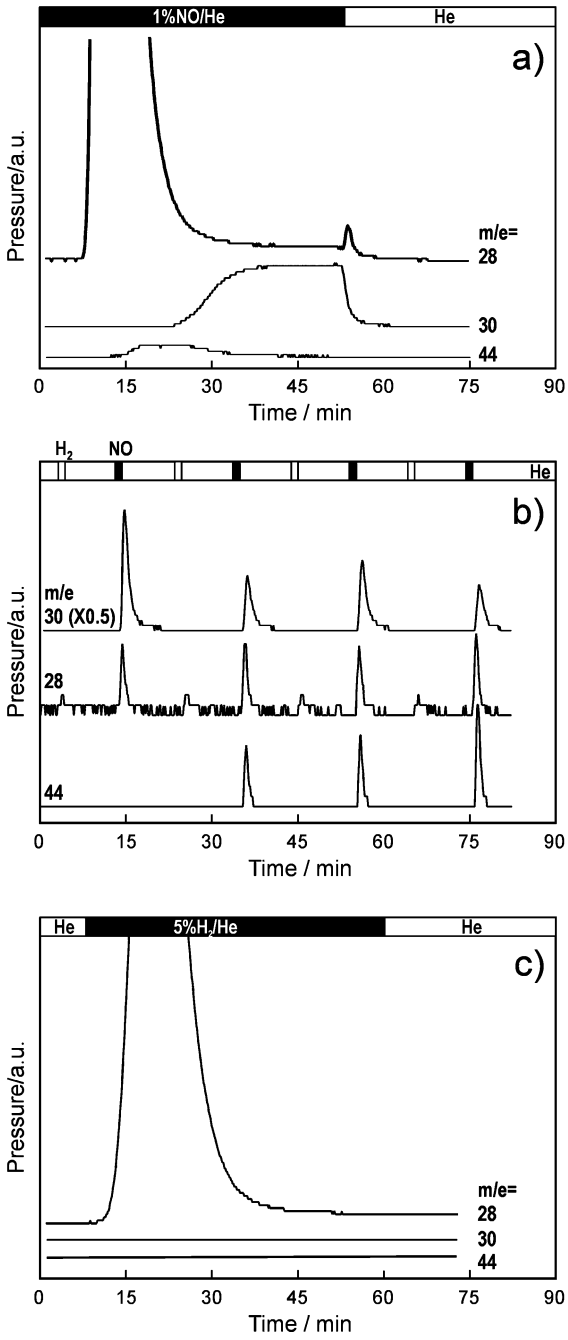

Figure 6. Mass signal profiles of $NO-H_2$ reactions over 1 wt % Pd/MnO_x-CeO_2 at 150 °C (reduced catalyst). (a) Continuous supply of 1% NO/He, followed by (b) the alternative $NO-H_2$ pulse reactions, and subsequent (c) continuous supply of 5% H_2/He.

(Figure 7a) would take place, whereas the second path (Figure 7b) would become dominant with an increasing amount of supplied H_2.

One may assume that the transport of adsorbed NO_x via surface or gas phase to Pd, where reactions with hydrogen would take place, is another possible interpretation of the present data. Supposing the NO_x adsorbates may diffuse on the surface to Pd, NO−TPD measurement should exhibit the desorption peaks at different temperatures for MnO_x-CeO_2 with and without Pd. In the present system, however, this is not the case, because the two NO desorption peaks at ca. 200 and 300 °C which were observed for MnO_x-CeO_2 were not affected by loading Pd.[9] The transfer of adsorbed NO_x via gas phase cannot explain the significant evolution of N_2, because the desorption of NO from MnO_x-CeO_2 in a stream of H_2 requires heating above 150 °C.[7]

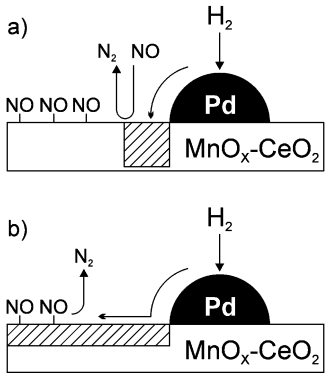

Figure 7. Possible two models for spillover-assisted $NO-H_2$ reaction over Pd/MnO_x-CeO_2 catalyst.

The proposed mechanisms (Figure 7) can work even in the presence of O_2. However, since part of H_2 must be consumed by combustion, the reduction of NO_x is still suppressed depending upon the O_2 partial pressure as shown in Figure 3. In addition, oxygen adsorption onto the anion vacancy in MnO_x-CeO_2 would also lead to negative effects on the reduction of NO. These considerations give an insight into the use of such a NO_x-adsorbing catalyst, i.e., this catalyst is more suitable for a process alternating sorptive NO removal and subsequent reduction by lean H_2, which has been first developed by Toyota,[4] rather than steady-state reactions. The experimental results for this type of NO_x catalyst will appear in our following publication soon.

Summary

Our previous studies indicated that the impregnation of Pd onto NO_x-adsorbing material, MnO_x-CeO_2, yields an efficient catalyst for selective $NO-H_2$ reaction at <150 °C in an excess O_2. The present study demonstrates convincing evidence to support the hypothesis that the role of impregnated Pd is to produce hydrogen atoms, which spill over onto the surface of MnO_x-CeO_2 and lead to the reduction of NO_x adsorbing thereon. The largest hydrogen-spillover in the present system occurred for the equimolar oxide, $0.5MnO_x-0.5CeO_2$, which exhibits the largest NO uptake via oxidative adsorption as NO_2^-/NO_3^-. The spilt-over hydrogen immediately gives rise to the anion vacancies on the surface of $0.5MnO_x-0.5CeO_2$, which are effective in reducing gaseous NO. There is also evidence provided that suggests that the spilt-over hydrogen can directly reduce all the nitrite species covering the surface of MnO_x-CeO_2.

References and Notes

(1) Arai, H.; Machida, M. *Catal. Today* **1994**, *22*, 97.

(2) Machida, M. In *Catalysis*; The Royal Society of Chemistry: Cambridge, 2000; Vol. 15, p 73.

(3) Miyoshi, N.; Matsumoto, S.; Katoh, K.; Tanaka, T.; Harada, J.; Takahashi, N.; Yokota, K.; Sugiura, M.; Kasahara, K. *SEA Paper* **1995**, 950809.

(4) Takahashi, N.; Shinjo, H.; Iijima, T.; Suzuki, T.; Yamazaki, K.; Yokota, K.; Suzuki, H.; Miyoshi, N.; Matsumoto, S.; Tanizawa, T.; Tanaka, T.; Tateishi, S.; Kasahara, K. *Catal. Today* **1996**, *27*, 63.

(5) Eguchi, K.; Watabe, M.; Ogata, S.; Arai, H. *J. Catal.* **1996**, *158*, 420.

(6) Hodjati, S.; Bernhardt, P.; Petit, C.; Pitchon, V.; Kinennemann, A. *Appl. Catal. B: Environ.* **1998**, *19*, 221.

(7) Friedell, E.; Skoglundh, M.; Westerberg, B.; Johansson, S; Smedler, G. *J. Catal.* **1999**, *196*, 183.

(8) Lietti, L.; Forzatti, P.; Nova, I.; Tronconi, S. *J. Catal.* **2001**, *204*, 175.

(9) Machida, M. *Catal. Survey Jpn.* **2002**, *4*, 91.
(10) Machida, M.; Uto, M.; Kurogi, D.; Kijima, T. *Chem. Mater.* **2000**, *12*, 3158.
(11) Machida, M.; Kurogi, D.; Kijima, T. *Chem. Mater.* **2000**, *12*, 3165.
(12) Machida, M.; Kurogi, D.; Kijima, T. *Stud. Surf. Sci. Catal.* **2001**, *138*, 267.
(13) Machida, M.; Uto, M.; Kurogi, D.; Kijima, T. *J. Mater. Chem.* **2001**, *11*, 900.
(14) Sermon, P. A.; Bond, G. C. *Catal. Rev.* **1973**, *8*, 211.
(15) Gruber, H. L. *Anal. Chem.* **1962**, *34*, 1828.
(16) Hicks, R. F.; Yen, Q. J.; Bell, A. T. *J. Catal.* **1984**, *89*, 498.
(17) Benson, J. E.; Hwang, H. S.; Boudart, M. *J. Catal.* **1973**, *30*, 146.
(18) Ryudin, Y. A.; Hicks, R. F.; Bell, A. T. Yermakov, Y. I. *J. Catal.* **1981**, *70*, 287.
(19) Nakamoto, K. In *Infrared and Raman Spectra of Inorganic and Coordination Compounds*, 4th ed.; Wiley: New York, 1986.
(20) Klingenberg, B.; Vannice, M. A. *Appl. Catal., B: Environ.* **1999**, *21*, 19.
(21) Huang, S. J.; Walters, A. B.; Vannice, M. A. *Appl. Catal., B: Environ.* **2000**, *26*, 101.
(22) Meunier, F. C.; Zuzaniuk, V.; Breen, J. P.; Olsson, M.; Ross, J. R. H. *Catal. Today* **2000**, *59*, 287.
(23) Martinez-Arias, A.; Soria, J.; Consesa, J. C.; Seoane, X. L.; Arcoya, A.; Cataluna, R. *J. Chem. Soc., Faraday Trans.* **1995**, *91*, 1679.